

## Intermediate valence behaviour of Yb in a new intermetallic compound $\text{YbNi}_{0.8}\text{Al}_{4.2}$

This article has been downloaded from IOPscience. Please scroll down to see the full text article.

2006 J. Phys.: Condens. Matter 18 10353

(<http://iopscience.iop.org/0953-8984/18/46/004>)

View [the table of contents for this issue](#), or go to the [journal homepage](#) for more

Download details:

IP Address: 129.252.86.83

The article was downloaded on 28/05/2010 at 14:30

Please note that [terms and conditions apply](#).

# Intermediate valence behaviour of Yb in a new intermetallic compound $\text{YbNi}_{0.8}\text{Al}_{4.2}$

V H Tran<sup>1,4</sup>, W Miiller<sup>1</sup>, A Kowalczyk<sup>2</sup>, T Toliński<sup>2</sup> and G Chełkowska<sup>3</sup>

<sup>1</sup> W Trzebiatowski Institute of Low Temperature and Structure Research, Polish Academy of Sciences, PO Box 1410, 50-950 Wrocław, Poland

<sup>2</sup> Institute of Molecular Physics, Polish Academy of Sciences, Smulochowskiego 17, 60-179 Poznań, Poland

<sup>3</sup> Institute of Physics, University of Silesia, Uniwersytecka 4, 40-007 Katowice, Poland

E-mail: [V.H.Tran@int.pan.wroc.pl](mailto:V.H.Tran@int.pan.wroc.pl)

Received 18 April 2006, in final form 5 October 2006

Published 3 November 2006

Online at [stacks.iop.org/JPhysCM/18/10353](http://stacks.iop.org/JPhysCM/18/10353)

## Abstract

We report on the valence band electronic structure as well as structural, magnetic and electronic transport properties of a novel intermetallic  $\text{YbNi}_{0.8}\text{Al}_{4.2}$ . The compound crystallizes in the orthorhombic  $\text{YNiAl}_4$ -type structure ( $a = 4.049(2)$ ,  $b = 15.305(5)$  and  $c = 6.586(3)$  Å) with space group  $Cmcm$ . The valence band spectrum and magnetic data indicate an intermediate valency of Yb ions in the studied compound with a valence of about 2.66 at room temperature. The temperature dependences of electrical resistivity, Hall effect and thermoelectric power display characteristic features of Kondo lattice with a large Kondo temperature ( $\sim 1300$  K), being consistent with the intermediate valence scenario. An analysis of magnetic data suggests the presence of strong ferromagnetic correlations in the investigated compound at low temperatures. In order to obtain information about the electron–hole analogy between the Ce and Yb compounds, we have compared the observed behaviour with that of the dense Kondo compound  $\text{CeNiAl}_4$ .

(Some figures in this article are in colour only in the electronic version)

## 1. Introduction

Amongst intermetallic lanthanides, there exists a class of compounds in which the rare earth atoms such as Ce, Sm, Eu or Yb show a noninteger valency [1, 2]. The underlying physics of this phenomenon is governed by a hybridization between the 4f and conduction band states. Owing to a nearness of the 4f electron level to the Fermi energy, the hybridization easily leads to fluctuations of both charges and spins of these f electrons. In other words, the atoms may spend

<sup>4</sup> Author to whom any correspondence should be addressed.

an appreciable fraction of their time in two different electronic configurations, nonmagnetic  $f^n$  ones and magnetic  $f^m$  ones. This means that the occupation number  $n_f$  of such  $f$  states is less than one, and it changes dynamically with temperature. There exist about at least two models that attempt to explain the electronic properties of intermediate valence (IV) compounds. On the one hand, in the so-called interconfigurational fluctuation (ICF) model [3], the valence of the magnetic ions depends both on the energy difference  $E_{\text{ex}}$  of these states and on a characteristic fluctuation temperature,  $T_{\text{sf}}$ , that describes the dynamics of the fluctuations. As a consequence, a maximum at  $T_{\text{max}}$  occurs in the temperature dependence of the susceptibility. Furthermore, at relatively high temperatures, where the all atoms tend to occupy the magnetic  $f^m$  state (the  $f$  occupation number tends to unity), the magnetism appears to be typical of local moment. On the other hand, in terms of the Kondo–Anderson model (KAM) [4–6] the electronic properties of IV compounds may be described with help of the hybridization characterized by the hybridization strength  $V$ , which affects both the exchange interaction  $J_{\text{sf}}$  [3] and the width of the conduction band  $W$ . These quantities ascertain the appearance of a low-energy peak in the renormalized density of states of a characteristic Kondo temperature  $T_{\text{K}}$ . The thermodynamic properties of IV compounds reflect the temperature behaviour of  $n_f$  as well as the Kondo temperature  $T_{\text{K}}$ .

It is interesting to add that Yb-based compounds with the nonmagnetic  $f^{14}$  and magnetic  $f^{13}$  configurations may be regarded as the ‘ $f$ -hole’ analogue of Ce compounds, for which there are nonmagnetic  $f^0$  and magnetic  $f^1$  configurations. If the roles of the  $4f$  electron and  $4f$  hole are interchanged one observes similar phenomena, such as intermediate valence or heavy-fermion behaviour in Ce and Yb counterparts [7–9]. Previously, CeNiAl<sub>4</sub> was reported to exhibit properties typical of a dense Kondo or heavy-fermion (HF) system [10, 11]. The magnetic susceptibility that follows the Curie–Weiss law in the range 100–300 K suggests localized  $4f$  electron character. On the other hand, the electronic specific heat coefficient is estimated to be 204 mJ mol<sup>-1</sup> K<sup>-2</sup>, indicating the HF state at low temperatures. The resistivity shows  $\ln T$  dependence in the high-temperature regime and a broad maximum at around 120 K. The thermoelectric power is positive and exhibits a broad maximum at about 75 K [12] or at about 150 K [13]. In the context of the electron–hole analogy we thought it would be worth investigating the magnetic properties of YbNiAl<sub>4</sub>. The crystal structure of YbNi<sub>0.8</sub>Al<sub>4.2</sub> has not yet been reported, though other compounds RNiAl<sub>4</sub> (R = rare earth) are known to form a large series of compounds adopting the orthorhombic YNiAl<sub>4</sub>-type structure [14]. The physical properties of two of them, namely, of CeNiAl<sub>4</sub> [10–13, 15] and PrNiAl<sub>4</sub> [16, 17], have been investigated over the past decade, but nothing has been reported so far on other members of the series.

In this work, we report the crystal structure and valence band spectrum analysis, as well as the results of dc magnetization, electrical resistivity, Hall effect and thermoelectric power measurements on a new intermetallic compound of approximate stoichiometry YbNi<sub>0.8</sub>Al<sub>4.2</sub>. We show that YbNi<sub>0.8</sub>Al<sub>4.2</sub> crystallizes in the orthorhombic YNiAl<sub>4</sub>-type structure, isostructural to CeNiAl<sub>4</sub>, and shows IV behaviour.

## 2. Experimental details

Two polycrystalline samples were prepared by an induction melting of stoichiometric elements (Yb:Ni:Al = 1:1:4) in a water-cooled crucible in an inert atmosphere of argon. Due to the volatile nature of Yb at high temperatures, a weighed amount of Yb was taken with an excess of 5%. The purity of starting materials was 3 N Yb, 4 N Ni and 5 N Al. The weight losses after melting were less than 1%. The obtained samples were stable against air and moisture. No sign of decomposition was observed after several months. The quality and purity of the

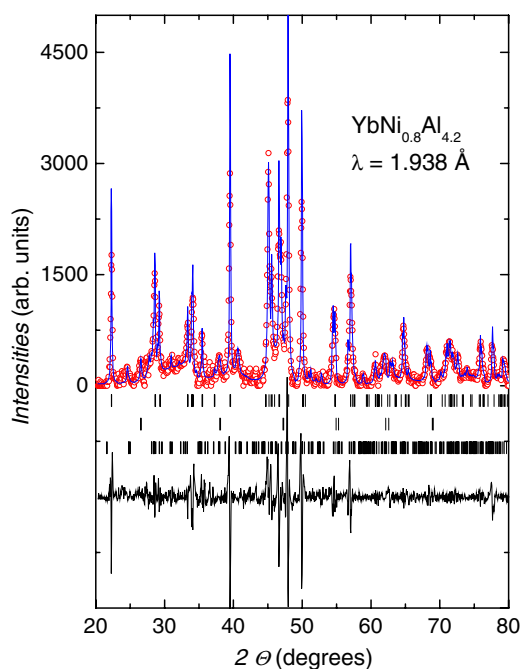


**Figure 1.** X-ray powder diffraction pattern of  $\text{YbNi}_{0.8}\text{Al}_{4.2}$  (open circles). The solid line presents the theoretical curve. The vertical lines indicate the positions of the Bragg reflections for  $\text{YbNi}_{0.8}\text{Al}_{4.2}$ ,  $\text{YbAl}_3$  and  $\text{Yb}_3\text{Ni}_5\text{Al}_{19}$ , respectively. The solid line at the bottom is the difference between the experimental and theoretical curves.

samples were checked by microscopic and x-ray diffraction analysis. An energy-dispersive x-ray analysis with a Philips EDX515-PV9800 scanning electron microscope indicated a main phase with the composition 16.53 Yb%, 13.15 Ni% and 70.32 Al%, corresponding to the stoichiometry 1:0.8:4.2. Therefore, in the following we assume that the stoichiometry of the studied compound is  $\text{YbNi}_{0.8}\text{Al}_{4.2}$ . Unfortunately, there exists in the studied samples a minor impurity (less than 3%), which can be identified as  $\text{YbAl}_3$  and  $\text{Yb}_3\text{Ni}_5\text{Al}_{19}$ . X-ray powder diffraction measurements were carried out at room temperature using  $\text{Fe K}\alpha$  radiation. The pattern obtained is given in figure 1. As can be seen, the Bragg reflections of the main phase can be indexed by an orthorhombic cell (space group  $Cmcm$ ) with the  $\text{YNiAl}_4$ -type structure [18] (figure 1), suggesting that a fraction of the Al atoms possibly occupies Ni positions in the structure. Obviously, further structural studies on a single crystal are needed to confirm this suggestion. Nevertheless, we may quote the crystallographic data of  $\text{CeNiAl}_4$  [12], for which the single crystal refinements yielded an occupation of C or N atoms at the 4c position, leading the material to possess the stoichiometry  $\text{CeNiAl}_4\text{C}_{0.7}$ . The lattice parameters of  $\text{YbNi}_{0.8}\text{Al}_{4.2}$  at room temperature were calculated by the least squares method [19] to be  $a = 4.049(2)$ ,  $b = 15.305(5)$  and  $c = 6.586(3)$  Å. In addition to the reflections of  $\text{YbNi}_{0.8}\text{Al}_{4.2}$  there are several visible peaks derived from the impurity phases  $\text{YbAl}_3$  and  $\text{Yb}_3\text{Ni}_5\text{Al}_{19}$ . These compounds crystallize in cubic (space group  $Pm\bar{3}m$  [20]) and orthorhombic (space group  $CmCm$  [21]) structures, respectively. The fitting of the diffraction pattern yielded  $a = 4.202$  Å for  $\text{YbAl}_3$  and  $a = 4.073(2)$ ,  $b = 16.091(5)$  and  $c = 27.099(6)$  Å for  $\text{Yb}_3\text{Ni}_5\text{Al}_{19}$ . The lattice parameters for the latter compound are a little larger than the literature data ( $a = 4.0635$ ,  $b = 15.901$  and  $c = 26.983$  Å) [21].

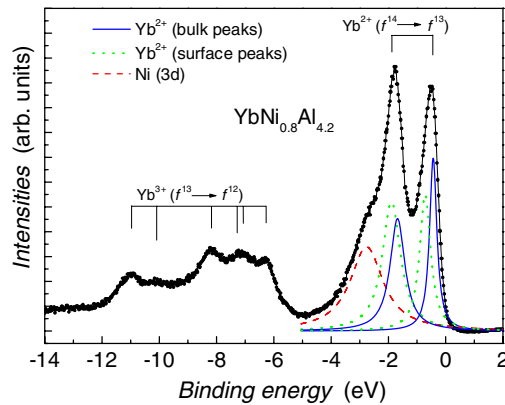


**Figure 2.** Valence band photoemission of  $\text{YbNi}_{0.8}\text{Al}_{4.2}$  measured at room temperature. The spectrum shows two sets of peaks derived from  $\text{Yb}^{3+}$ , and  $\text{Yb}^{2+}$  and the Ni 3d states.

An x-ray photoemission experiment was performed with monochromatized Al  $K\alpha$  radiation at room temperature using a PHI 5700/660 ESCA spectrometer. The valence band spectrum was collected immediately after breaking the samples in a vacuum of  $10^{-10}$  Torr. The Fermi level referred to was of the gold 4f level (84 eV). Magnetization ( $M$ ) measurements were performed on powdered samples in the temperature range 2–400 K and in magnetic fields up to 5 T using a commercial Quantum Design MPMS-5 magnetometer, and in fields up to 9 T using the MagLab2000 instrument. Electrical resistivity ( $\rho$ ) measurements were carried out on rectangular samples of uniform thickness  $1 \times 1 \times 5 \text{ mm}^3$  in the temperature range 2–300 K using a standard four-probe dc technique. The Hall coefficient ( $R_H$ ) was measured in magnetic fields up to 7 T in the temperature range 2–300 K. The thermoelectric power (TEP) was measured in the temperature range 4–300 K, using a differential method.

### 3. Results and discussion

#### 3.1. Valence band spectrum data

Figure 2 shows the valence spectrum for  $\text{YbNi}_{0.8}\text{Al}_{4.2}$ . The noticeable feature of the spectrum is the presence of two sets of peaks ranging between  $-4 \text{ eV}$  and  $E_F$ , and between  $-12$  and  $-5 \text{ eV}$ , respectively. The first set of peaks could be attributed to the superposition of the Ni 3d state and the spin–orbit doublet of the divalent Yb. In fact, the  $\text{Yb}^{2+} 4f_{7/2}$  peak with its spin–orbit partner  $4f_{5/2}$  are located at  $-0.44 \text{ eV}$  and at  $-1.68 \text{ eV}$ , respectively. These peaks can be identified as the bulk doublet and are deconvoluted as solid lines in figure 2. The spin–orbit splitting in  $\text{YbNi}_{0.8}\text{Al}_{4.2}$  is about 1.24 eV, which is comparable to the case of  $\text{YbAl}_3$  (1.27 eV) [22]. We distinguish another doublet at  $-1.91$  and  $-0.71 \text{ eV}$  originating from the surface  $4f_{7/2}$ – $4f_{5/2}$  transition (dotted lines). One can compare the x-ray photoelectron spectroscopy (XPS) data with those of  $\text{CeNiAl}_4$  [23]. For the latter compound a double-peak structure is observed: one peak is located at about 0.25 eV and the other at about 0.05 eV below  $E_F$ . The nearness of these peaks to the Fermi level points to stronger electron correlations in the  $\text{CeNiAl}_4$  case. In figure 2 the broad peak at  $-2.76 \text{ eV}$  is certainly due to the Ni 3d states (dashed line). We must point out that the energy position of the Ni 3d structure in the XPS valence band of  $\text{YbNi}_{0.8}\text{Al}_{4.2}$  is considerably shifted from the Fermi level, if one compares to that of the pure Ni metal ( $-0.4 \text{ eV}$  [24]). A larger shift of the Ni 3d band was observed for  $\text{CeNiAl}_4$  too [23]. Such

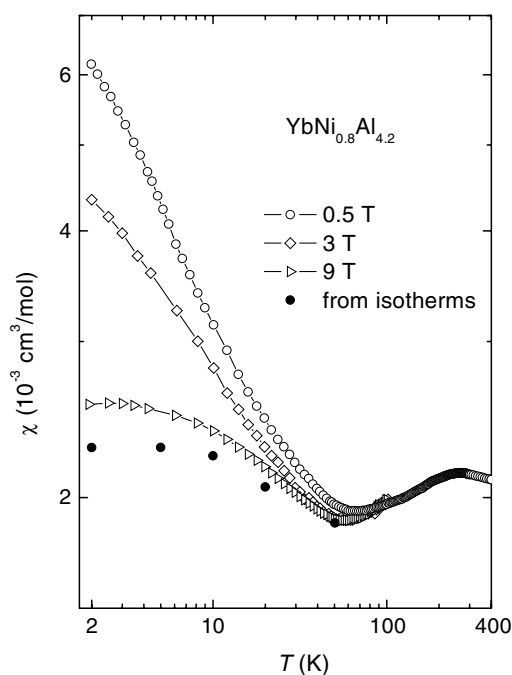


**Figure 3.** Temperature dependence of the magnetic susceptibility of  $\text{YbNi}_{0.8}\text{Al}_{4.2}$  measured at 0.5, 3 and 9 T (line + symbols). The solid circles are estimated high-field  $\chi_{\text{HF}}$  data.

a behaviour may be qualitatively understood by taking into account the 3d band-filling effect. As was demonstrated in the XPS experiment for Ni–Al alloys [24], with increasing Al content across the series Ni,  $\text{Ni}_3\text{Al}$ , NiAl,  $\text{Ni}_2\text{Al}_3$  and  $\text{NiAl}_3$ , the position due to the 3d states shifts down to large binding energies of 0.6, 0.9, 1.8, 1.9 and 2.5, respectively. This situation could happen in  $\text{YbNi}_{0.8}\text{Al}_{4.2}$  because of a higher 3d band filling caused by the relatively large Al content in the compound. Consequently, the energies of Ni states in  $\text{YbNi}_{0.8}\text{Al}_{4.2}$  and in  $\text{NiAl}_3$  with respect to  $E_{\text{F}}$  are not so different, and this would indicate that the 3d bands in these alloys are basically filled. The presence of the Ni 3d and Yb 4f states near the Fermi level implies a high density of the hybridized f–d band.

The structure between  $-12$  and  $-5$  eV below  $E_{\text{F}}$  can be recognized as the multiplet due to the  $4f^{13} \rightarrow 4f^{12}$  transition. Apparently, the intensity of the  $\text{Yb}^{3+}$  part is comparable with that of the bulk  $\text{Yb}^{2+}$  part, suggesting that the Yb atoms in the studied alloy are in an intermediate valence state. For  $\text{YbNi}_{0.8}\text{Al}_{4.2}$ , the valence  $\nu$  of Yb was estimated from the intensity ratio of the trivalent part and the bulk divalent part, and it amounts to about 2.66(2).

### 3.2. Magnetic properties

The magnetic susceptibility  $\chi \equiv M(T)/H$  of  $\text{YbNi}_{0.8}\text{Al}_{4.2}$  in several magnetic fields  $H$  as a function of temperature is shown in figure 3. The  $\chi(T)$  curve does not exhibit Curie–Weiss behaviour in the temperature range measured. Instead, it displays a broad maximum around  $T_{\text{max}}^{\chi} = 250$  K, corroborating the intermediate valence behaviour of the Yb atom in  $\text{YbNi}_{0.8}\text{Al}_{4.2}$ . According to Hundley *et al* [25], the value of  $T_{\text{max}}^{\chi}$  is believed to scale with the coherence temperature  $T_{\text{coh}}$  by the relation  $T_{\text{coh}} \propto 4T_{\text{max}}^{\chi}/(2J + 1)$ . From this relationship, and taking  $J = 7/2$  for  $\text{Yb}^{3+}$ , we estimate  $T_{\text{coh}} \sim 125$  K for  $\text{YbNi}_{0.8}\text{Al}_{4.2}$ . Such a large observed

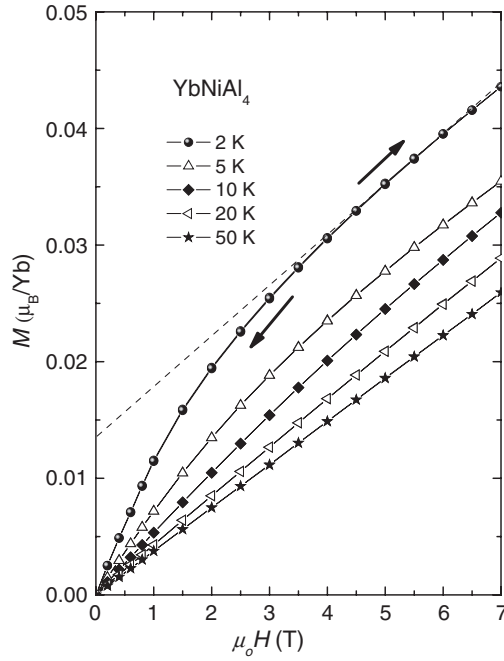


**Figure 4.** Magnetization of  $\text{YbNi}_{0.8}\text{Al}_{4.2}$  as a function of applied magnetic field. The dashed line shows an estimate of the high-field susceptibility  $\chi_{\text{HF}}$  at 2 K. The arrows indicate field directions for which the magnetization data were recorded.

value of  $T_{\text{max}}^{\chi}$  is presumably due to a strong hybridization of the 4f electrons with the conduction electrons, and it corresponds to IV systems with a large Kondo temperature. For intermediate valence materials, Rajan, within the Coqblin–Schrieffer model, predicted [26] a maximum in the temperature dependence of magnetic susceptibility at a temperature of approximately  $(0.3\text{--}0.5)T_0$  for  $J > 1/2$ , where  $T_0$  is the characteristic spin-fluctuation temperature. From the data presented in figure 3, we can evaluate  $T_0 \sim 625$  K. Using the relationship between  $T_0$  and  $T_K$  ( $T_0 = (2J + 1)T_L/2\pi$  [26] and  $T_K = 0.6745T_L$  [27]), we find the Kondo temperature  $T_K \sim 1325$  K for  $\text{YbNi}_{0.8}\text{Al}_{4.2}$ . Rajan [26] also predicted the relationship between the electronic specific heat coefficient  $\gamma$  and  $T_0$  by the relation  $\gamma = 2J\pi k_B/6T_0$ . From this we would expect the  $\gamma$ -value of  $\text{YbNi}_{0.8}\text{Al}_{4.2}$  to attain  $22 \text{ mJ mol}^{-1} \text{ K}^{-2}$ .

As can be seen in figure 3,  $\chi(T)$  below 50 K is strongly temperature and field dependent. With decreasing temperature  $\chi(0.5 \text{ T}, T)$  reaches a value as large as  $6.2 \times 10^{-3} \text{ cm}^3 \text{ mol}^{-1}$  at 2 K. The application of magnetic fields suppresses the magnitude of the low-temperature susceptibility. However, the upturn feature of the  $\chi(T)$  curves persists at a high field of 9 T. Even the high-field susceptibility  $\chi_{\text{HF}}$  (solid points), obtained from the linear part of the isotherms (see figure 4), displays a similar behaviour. Such field and temperature dependences of the susceptibility at low temperatures do not merit an interpretation in terms of IV model, and rather indicate strong ferromagnetic correlations.

Figure 4 shows isothermal magnetization curves  $M(H)$  measured at several temperatures below 50 K. The data do not show any saturation in fields up to 7 T. Also, we could not detect any hysteresis. These features suggest that the short-range correlation in  $\text{YbNi}_{0.8}\text{Al}_{4.2}$  is intrinsic. A strong field dependence of  $M(H)$  can be interpreted as being due to two components. The first one is the contribution of the intrinsic magnetic moments of magnetic

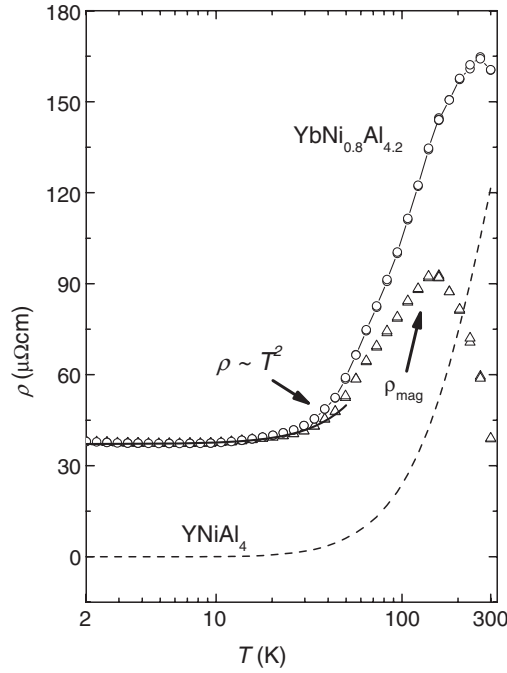


**Figure 5.** Temperature dependence of the electrical resistivity of  $\text{YbNi}_{0.8}\text{Al}_{4.2}$  (circles + line) and  $\text{YNiAl}_4$  (dashed line). The triangles represent the magnetic resistivity of  $\text{YbNi}_{0.8}\text{Al}_{4.2}$ .

ions, which provide a linear dependence of the  $M(H)$  curves at high fields and low temperatures. The slope of the linear part of the magnetization may be defined as the high-field susceptibility  $\chi_{\text{HF}}$ . The second component is reflected by a saturable portion of the magnetization and presumably is associated with magnetic correlations between those moments. The contribution of the second component,  $M_s$ , can be estimated from the intercept of the dashed line to the vertical axis.

### 3.3. Electronic transport properties

The electrical resistivity of  $\text{YbNi}_{0.8}\text{Al}_{4.2}$  and  $\text{YNiAl}_4$  as a function of temperature is displayed in figure 5. It can be seen that the resistivity of  $\text{YNiAl}_4$  is a typical behaviour of ordinary metals. On the other hand,  $\rho(T)$  of  $\text{YbNi}_{0.8}\text{Al}_{4.2}$ , with a broad maximum at around 270 K and the Fermi liquid temperature dependence ( $\rho \propto T^2$ ) at low temperatures, suggests the behaviour of a concentrated Kondo compound with a large Kondo temperature  $T_K$ . The magnetic contribution  $\rho_{\text{mag}}$  to the resistivity of  $\text{YbNi}_{0.8}\text{Al}_{4.2}$  was estimated by subtracting the phonon-induced resistivity as measured in the reference material  $\text{YNiAl}_4$ . The maximum appearing at about  $T_{\text{max}}^\rho = 160$  K in the  $\rho_{\text{mag}}(T)$  curve may evidence the onset of coherent scattering of the conduction electrons from Kondo centres arranged periodically on the lattice, since it is close to the coherence temperature evaluated above (125 K). In figure 5 we also show the fit of the magnetic resistivity data for temperatures between 2 and 50 K (solid line) to the relation  $\rho_{\text{mag}}(T) = \rho_0 + AT^2$ . The fit yielded a temperature coefficient of the resistivity  $A = 5.1 \times 10^{-3} \mu\Omega \text{ cm K}^{-2}$  and the residual resistivity  $\rho_0$  of  $37 \mu\Omega \text{ cm}$ . The deduced coefficient  $A$  of  $\text{YbNi}_{0.8}\text{Al}_{4.2}$  is similar to those observed for  $\text{YbInAu}_2$  [28] and  $\text{YbNi}_2\text{Ge}_2$  [29].



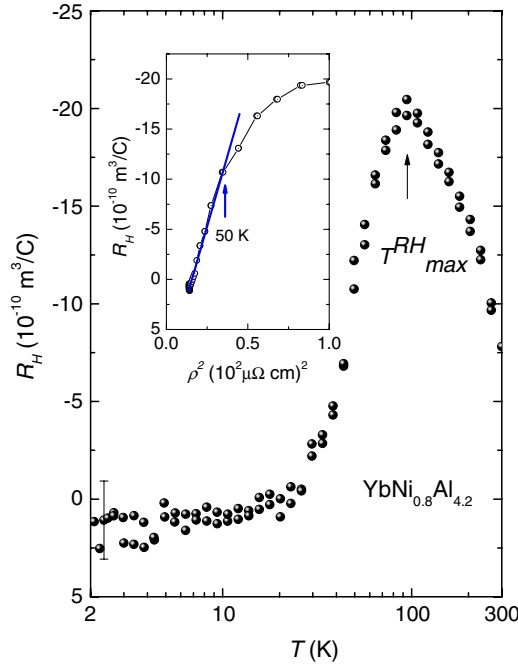


**Figure 6.** Temperature dependence of the Hall coefficient of  $\text{YbNi}_{0.8}\text{Al}_{4.2}$  measured at 7 T. The inset displays the linear dependence between  $R_H$  and  $\rho^2$  below 50 K.

Both the latter compounds were found to show an enhanced electronic coefficient of the specific heat  $\gamma$ , i.e., of 40 and 136  $\text{mJ mol}^{-1} \text{K}^{-2}$ , respectively. The enhanced values of the coefficients  $A$  and  $\gamma$  in these materials were shown to associate with the enhancement of the electron effective mass [28]. For most Yb-based intermetallics, the Kadowaki–Woods relation  $A/\gamma^2$  was found to range from  $0.4 \times 10^{-6}$  to  $0.8 \times 10^{-5} \mu\Omega \text{ cm mol}^2 \text{K}^2 \text{mJ}^{-2}$  [28]. Assuming this relation to be valid for  $\text{YbNi}_{0.8}\text{Al}_{4.2}$  one approximates  $\gamma$  to locate between 25 and 113  $\text{mJ mol}^{-1} \text{K}^{-2}$ , being the same order of magnitude as that estimated from the magnetic susceptibility data (22  $\text{mJ mol}^{-1} \text{K}^{-2}$ ).

The Hall coefficient  $R_H$  of  $\text{YbNi}_{0.8}\text{Al}_{4.2}$  as a function of temperature is shown in figure 6. The Hall coefficient is generally negative. This finding, along with the negative thermoelectric power (see below), suggests the dominant contribution of the negative charge carriers. Inspection of the temperature dependence of the Hall coefficient indicates some similarities to typical Kondo lattices or heavy-fermion compounds [30–32], namely there are remarkable values of  $R_H$  and a broad extremum in the  $R_H(T)$ -dependence. As for strongly correlated electron systems, the temperature dependence of  $R_H$  is mainly determined by skew scattering [32, 33]. At low temperatures, the skew scattering from the magnetic ions may give a relationship  $R_H \propto \rho^2$  [33]. Such a behaviour has been found for a few heavy-fermion compounds at temperatures below  $T_{\text{max}}^{\text{RH}}$  [33]. For  $\text{YbNi}_{0.8}\text{Al}_{4.2}$  we observe a linear dependence between  $R_H$  and  $\rho^2$  below 50 K, i.e., about  $T_{\text{max}}^{\text{RH}}/2$  (see the inset of figure 6).

Pursuing the temperature dependence of the Hall coefficient, we may note that the appearance of the  $T_{\text{max}}^{\text{RH}}$  maximum is commonly interpreted as being due to vanishing of incoherent skew scattering and development of coherent scattering below  $T_{\text{max}}^{\text{RH}}$ . Thus, the position of  $T_{\text{max}}^{\text{RH}}$  defines the coherence temperature. However, as regards  $\text{YbNi}_{0.8}\text{Al}_{4.2}$ ,

$T_{\max}^{\text{RH}} = 95$  K is smaller than  $T_{\text{coh}}$  deduced from the magnetic susceptibility and resistivity measurements. Note that  $T_{\max}^{\text{RH}}$  of some Yb-based intermediate valent compounds, e.g. YbCuAl and YbCu<sub>2</sub>Si<sub>2</sub>, also occurs at temperatures lower than their  $T_{\max}^{\rho}$  [34]. This discrepancy with the theory developed for Ce-based compounds [32] suggests that for Yb-based compounds one must take into account, in addition to incoherent and coherent skew scattering mechanisms, other factors, for instance the Kondo hole effect or the large ground state degeneracy ( $N = 2J + 1$ ). The first effect results from imperfections in the Yb sublattice. In normal metals such lattice defects alter mainly the residual resistivity. In Kondo lattices, however, the defect on a given site influences the Kondo resonance, playing a role like a Kondo hole in analogy to the case of magnetic impurity in a nonmagnetic matrix [35]. The presence of the Kondo hole effect has been documented in several Yb-based intermetallics, like YbCu<sub>4</sub>Ag [36], YbCu<sub>2</sub>Si<sub>2</sub> [37] and YbNi<sub>2</sub>Ge<sub>2</sub> [29]. As an effect of the Kondo hole, an additional contribution  $\rho^{\text{KH}} = \rho_0^{\text{KH}} - BT^2$  to the total resistivity will modify both the residual resistivity and the  $T^2$ -coefficient of the resistivity [35]. Thus, the coherent temperature can be shifted to higher temperatures compared to that of the system without a Kondo hole. The ground state degeneracy is a second mechanism that may be the reason for the difference in magnetic behaviour between Ce- and Yb-based intermetallics. As is predicted by Rajan [26], the density of states (DOS) has a peak situated above the Fermi level ( $E_{\text{F}}$ ) for  $N \geq 4$  but it is located just at  $E_{\text{F}}$  for  $N \leq 3$ . This means that the DOS of the conduction band for Ce-based compounds can be more enhanced by many-body correlations compared to that for Yb-based compounds. Comparison of the XPS data presented here with those of CeNiAl<sub>4</sub> [23] may confirm the theoretical prediction. It is of interest to recall that the Kondo hole, ground state degeneracy and other mechanisms like single-body band effect and intersite magnetic correlation have recently been considered to be factors causing the difference in  $A/\gamma^2$  ratio between the Ce- and Yb-based compounds [28].

In figure 7 we show the temperature dependence of the thermoelectric power  $S(T)$  of YbNi<sub>0.8</sub>Al<sub>4.2</sub>. The TEP of YbNi<sub>0.8</sub>Al<sub>4.2</sub> is negative over the whole range of temperature. This fact is in contrast to the Kondo lattice compound CeNiAl<sub>4</sub>, for which  $S(T)$  was reported to be positive [12, 13]. The opposite signs in the thermoelectric power of the Ce and the Yb co-partners may reflect the electron-hole symmetry of the 4f<sup>1</sup> (Ce) and 4f<sup>13</sup> (Yb) states. Analogous observations were reported for a large number of Ce and Yb compounds [38]. As can be seen from figure 7, two well formed extrema are present in the  $S(T)$  curve: one is located at about 40 K and the other is at 270 K. Therefore, the overall behaviour of the TEP of YbNi<sub>0.8</sub>Al<sub>4.2</sub> is consistent with the prediction of the theory presented by Zlatić *et al* for Ce- and Yb-based intermetallics [39].

The observed high-temperature TEP maximum at  $T_{\max}^S = 270$  K correlates well with the maximum of the susceptibility and resistivity and is possibly explained by the Kondo effect. A comparison of  $T_{\max}^S$  with that of CeNiAl<sub>4</sub> (~75 K [12], ~150 K [13]) strongly indicates that the Kondo temperature of YbNi<sub>0.8</sub>Al<sub>4.2</sub> is much higher than that of CeNiAl<sub>4</sub>.

It is worthwhile noting that the TEP of YbNi<sub>0.8</sub>Al<sub>4.2</sub> has a large value of  $-50 \mu\text{V K}^{-1}$  at  $T_{\max}^S$ , which is quite comparable to those found in other intermediate valence compounds, like Yb<sub>2</sub>Pt<sub>3</sub>Sn<sub>5</sub> [40] and YbRh<sub>2</sub>Ga [41]. Such large  $S$ -values may be ascribed to the formation of a narrow peak in the electron state density near the Fermi level due to the correlation between the conduction electrons and the 4f electrons/holes of Ce/Yb ions, respectively [39].

In the inset of figure 7 we display the temperature dependence of thermoelectric power factor (TPF),  $S^2/\rho$ . At 35 K the TPF reaches  $45 \mu\text{W K}^{-2} \text{cm}^{-1}$ , comparable to the values found in Yb<sub>2</sub>Pt<sub>3</sub>Sn<sub>5</sub> of  $43 \mu\text{W K}^{-2} \text{cm}^{-1}$  at 13 K [40], NaCo<sub>2</sub>O<sub>4</sub> ( $50 \mu\text{W K}^{-2} \text{cm}^{-1}$ ) and Bi<sub>2</sub>Te<sub>3</sub> ( $40 \mu\text{W K}^{-2} \text{cm}^{-1}$ ) at room temperature [42]. The latter material is commonly used as a thermoelectric material.

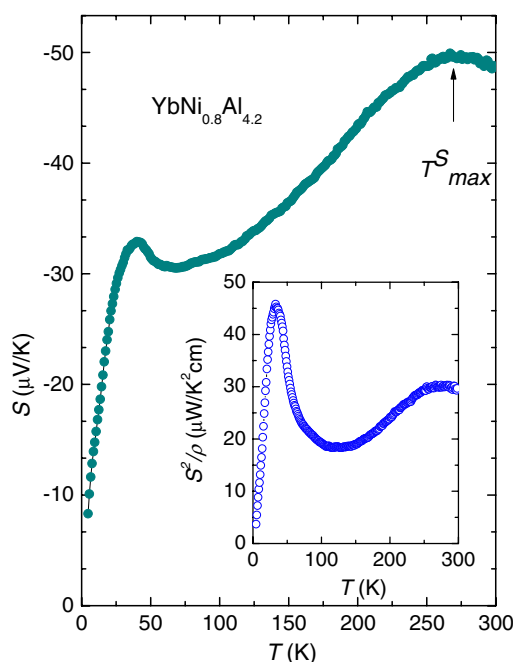


**Figure 7.** Temperature dependence of the thermoelectric power of  $\text{YbNi}_{0.8}\text{Al}_{4.2}$ . The inset shows the thermoelectric power factor as a function of temperature.

#### 4. Concluding remarks

We have synthesized a new intermetallic compound  $\text{YbNi}_{0.8}\text{Al}_{4.2}$  and characterized it by means of x-ray diffraction and microprobe EDX measurements. It appears that  $\text{YbNi}_{0.8}\text{Al}_{4.2}$  crystallizes in the orthorhombic  $\text{YNiAl}_4$ -type structure, being isostructural to that of the Kondo lattice compound  $\text{CeNiAl}_4$ . The physical property measurements indicate that  $\text{YbNi}_{0.8}\text{Al}_{4.2}$  is an intermediate valence compound with a characteristic Kondo temperature of about 1325 K and Yb valence of 2.66 at room temperature. Besides, it may be that in  $\text{YbNi}_{0.8}\text{Al}_{4.2}$  strong ferromagnetic correlations set in at temperatures below 50 K. Based on the XPS data we suggest that the role of Yb 4f–Ni 3d hybridization could be relevant for explaining the IV behaviour of  $\text{YbNi}_{0.8}\text{Al}_{4.2}$ . A comparison of electronic properties with those of  $\text{CeNiAl}_4$  suggests an electron–hole analogy. However, there exists a clear difference in regards to energy scale in these compounds. The investigated  $\text{YbNi}_{0.8}\text{Al}_{4.2}$  compound exhibits a larger Kondo temperature compared to that of  $\text{CeNiAl}_4$ . We have considered this difference in relation to the Kondo hole and ground state degeneracy effects.

#### Acknowledgment

One of us (TVH) is grateful for financial support from the Polish State Committee within grant No. 4T08A 045 24.

#### References

- [1] Varma C M 1976 *Rev. Mod. Phys.* **48** 219
- [2] Lawrence J M, Riseborough P S and Parks R D 1979 *Prog. Phys.* **44** 1
- [3] Sales B C and Wohlleben D K 1975 *Phys. Rev. Lett.* **35** 1240

- [4] Kondo J 1964 *Prog. Theor. Phys. Japan* **32** 37
- [5] Bickers N E, Cox D L and Wilkins J W 1987 *Phys. Rev. B* **36** 2036
- [6] Schlottman P 1989 *Phys. Rep.* **181** 1
- [7] Bickers N E, Cox D L and Wilkins J W 1985 *Phys. Rev. Lett.* **54** 230
- [8] Fujimori A, Shimizu T and Yasuoka H 1987 *Phys. Rev. B* **35** 8945
- [9] Patthey F, Imer J-M, Schneider W-D, Beck H, Baer Y and Delley D 1990 *Phys. Rev. B* **42** 8864
- [10] Mizushima T, Isikawa Y, Maeda A, Oyabe K, Mori K, Sato K and Kamigaki K 1991 *J. Phys. Soc. Japan* **60** 753
- [11] Mizushima T, Ishikawa Y, Mori K and Sakurai J 1996 *J. Phys. Soc. Japan* **65** (Suppl.) 146
- [12] Poduska K M, DiSalvo F J and Petříček V 2000 *J. Alloys Compounds* **308** 64
- [13] Ghoshray K, Bandyopadhyay B, Poddar A, Ghoshray A, Mukadam M D and Yusuf S M 2004 *Solid State Commun.* **132** 725
- [14] Parther E and Chabot B 1984 *Handbook on the Physics and Chemistry of Rare Earths* vol 6, ed K A Gschneidner Jr and L Eyring (Amsterdam: North-Holland) p 113
- [15] Ghoshray K, Bandyopadhyay B and Ghoshray A 2002 *Phys. Rev. B* **65** 174412
- [16] Mizushima T, Ishikawa Y, Sakurai J and Mori K 1995 *J. Magn. Magn. Mater.* **140–144** 925
- [17] Ghoshray K, Bandyopadhyay B and Ghoshray A 2004 *Phys. Rev. B* **69** 094427
- [18] Rykhal R M, Zarechnyuk O S and Yarmolyuk Y P 1972 *Sov. Phys.—Crystallogr.* **17** 453
- [19] Rodriguez-Carvajal J 1993 *Physica* **192** 55
- [20] Iandelli A and Palenzona A 1972 *J. Less Common Met.* **29** 293
- [21] Bauer E D, Bobev S, Thompson J D, Hundley M F, Sarro J L, Lobos A and Aligia A A 2004 *J. Phys.: Condens. Matter* **16** 4025
- [22] Oh S-J, Suga S, Kazaki A, Taniguchi M, Ishii T, Kang J-S, Allen J W, Gunnarsson O, Christensen N E, Fujimori A, Suzuki T, Kasuya T, Miyahara T, Kato H, Schönhammer K, Torikachvili M S and Maple M B 1988 *Phys. Rev. B* **37** 2861
- [23] Kashiwakura T, Okane T, Suzuki S, Sato S, Watanabe M, Harasawa A, Kinoshita T, Kakizaki A, Ishii T, Nakai S and Isikawa Y 2000 *J. Phys. Soc. Japan* **69** 3095
- [24] Fuggle J C, Hillebrecht F U, Zeller R, Żoźnierek Z, Bennett P A and Freiburg Ch 1982 *Phys. Rev. B* **27** 2145
- [25] Hundley M F, Canfield P C, Thompson J D, Fisk Z and Lawrence J M 1990 *Phys. Rev. B* **42** 6842 and references therein
- [26] Rajan V T 1983 *Phys. Rev. Lett.* **51** 308
- [27] Hewson A C and Rasul J W 1983 *J. Phys. C: Solid State Phys.* **16** 6799
- [28] Tsujii N, Yoshimura K and Kosuge K 2003 *J. Phys.: Condens. Matter* **15** 1993
- [29] Knebel G, Braithwaite D, Lapertot G, Canfield P C and Flouquet J 2001 *J. Phys.: Condens. Matter* **13** 10935
- [30] Onuki Y, Yamazaki T, Ukon I, Komatsubara T, Umezawa A, Kwok W K, Crabtree G W and Hinks D G 1989 *J. Phys. Soc. Japan* **58** 2119
- [31] Onuki Y, Yamazaki T, Omi T, Ukon I, Kobori A and Komatsubara T 1989 *J. Phys. Soc. Japan* **58** 2126
- [32] Fert A and Levy P M 1987 *Phys. Rev. B* **36** 1907
- [33] Kotani H and Yamada K 1994 *J. Phys. Soc. Japan* **63** 2627
- [34] Cattaneo E 1986 *Z. Phys. B* **64** 317
- [35] Lawrence J M, Thompson J D and Chen Y Y 1985 *Phys. Rev. Lett.* **54** 2537
- [36] Graf T, Movshovich R, Thompson J D, Fisk Z and Canfield P C 1995 *Phys. Rev. B* **52** 3099
- [37] Alami-Yadri K, Wilhelm H and Jaccard D 1998 *Eur. Phys. J. B* **6** 5
- [38] Zlatić V and Monnier R 2005 *Phys. Rev. B* **71** 165109
- [39] Zlatić V, Horvatić B, Milat I, Coqblin B, Czyczoll G and Grenzebach C 2003 *Phys. Rev. B* **68** 104432
- [40] Muro Y, Yamane K, Kim M S, Takabatake T, Godart C and Rogl P 2003 *J. Phys. Soc. Japan* **72** 1745
- [41] Chen G F, Sakamoto I, Ohara S, Takami T, Ikuta H and Mizutani U 2004 *Phys. Rev. B* **69** 054435
- [42] Terasaki I, Sasago Y and Uchinokura K 1997 *Phys. Rev. B* **56** R12685